

Red-green-blue Beam Combiner Based on Two-mode Interference

Youngchul Chung*

Department of Electronics and Communication Engineering, Kwangwoon University, Seoul 01897, Korea

(Received September 3, 2018 : revised December 8, 2018 : accepted December 10, 2018)

A compact red-green-blue beam combiner (multiplexer) based on two-mode interference (TMI) is proposed and its feasibility is shown through three-dimensional beam propagation simulation. The first stage TMI beam combiner makes red (637 nm) and blue (446 nm) beams combined toward one output port and the second stage one combines red, blue, and green (532 nm) beams. The power transmission to the output port from the red, green, and blue input ports are 0.96, 0.99, and 0.98, respectively. When the wavelength deviation is 10 nm, the transmission is maintained to be larger than 0.9. The size of the combiner is as tiny as $0.02 \times 3.8 \text{ mm}^2$.

Keywords : Red-green-blue beam combiner, Two-mode interference, Integrated optics, Pico-projectors
OCIS codes : (130.3120) Integrated optics devices; (230.7390) Waveguides, planar; (060.4230) Multiplexing; (090.2820) Heads-up displays

I. INTRODUCTION

The displays for smart phones are small-area flat panel types such as OLED (Organic Light Emitting Diode) and LCD displays of several square foot area. Therefore, a hand-held projector device for large image display (so called pico-projector) has been drawing lots of attention. A full-size image can be projected on a wall or a piece of paper with a pico-projector. Moreover, the scanned laser pico-projectors exhibit infinite focus which can be projected on a surface with three dimensional depth profiles.

Pico-projectors such as mobile projector, eyeglass projector, head-mount display, head-up display and virtual-retina display have been extensively researched [1, 2]. In particular, wearable computers equipped with an eyewear projector or a head-mount display have been developed actively. These mobile systems can overlay visual information generated by computer in the real world and provide the information immediately in a hands-free manner [3]. Therefore, the compact projector such as an eyeglass projector can open a new paradigm of augmented reality (AR) with wearable computer and provide useful tools for human society [4]. Even though the compact pico-projectors can be realized using liquid crystal display (LCD) with LED lighting and

they can be applied to head-mount displays [5], images can't be easily focused onto eyes in those kinds of LCD pico-projectors because they require very accurate lens systems. On the other hand, scanned laser image projectors can be easily applied to head-mount displays [6-8]. They are composed of a laser diode source, a red-green-blue (RGB) beam combiner and a laser scanner. The RGB colors from laser sources are combined into a white beam with beam combiner, scanned onto the screen by a laser scanner without the use of a complicated focusing lens system, and a color image can be obtained.

A head-up display (HUD), which enables drivers to recognize car speed or other information with small shift in eye direction, is steadily being introduced into the auto industry. At the same time, with the advent of smart phones that are capable of processing complex data and recognizing positions, augmented reality (AR) is becoming more and more practical and familiar. In some AR HUD navigation systems, drivers can experience epoch-making views in which AR information is superimposed on the background scenery [9, 10].

The conventional RGB beam combiner requires complicated lens and mirror systems, which exhibit the limitation in reducing its size. Recently, an integrated waveguide type

*Corresponding author: ychung@kw.ac.kr, ORCID 0000-0002-2460-2618

Color versions of one or more of the figures in this paper are available online.



This is an Open Access article distributed under the terms of the Creative Commons Attribution Non-Commercial License (<http://creativecommons.org/licenses/by-nc/4.0/>) which permits unrestricted non-commercial use, distribution, and reproduction in any medium, provided the original work is properly cited.

RGB beam combiner as tiny as a ‘grain of rice’ has been proposed, where specially designed directional couplers are properly cascaded [11]. In this paper, a new design of compact integrated waveguide RGB beam combiner based on a two-mode interference (TMI) effect [12, 13] is proposed. In the two-mode waveguide, the wavelength dependence of the propagation constants of two modes are different from each other, and the beating between two modes is wavelength-dependent, which can be used for beam combining (or multiplexing). Properly designed two-mode waveguides connected to converging and diverging directional couplers can combine (multiplex) RGB colors. In Section II, the operation principle of the TMI device is explained. In Section III, the design example of the RGB beam combiner is presented and the beam combining performances are confirmed by three-dimensional beam propagation simulation. The tolerance of the device under wavelength deviation is investigated and the effect of the waveguide width deviation, which might be inevitable during the fabrication process, is also investigated. Finally conclusions are given.

II. DEVICE STRUCTURE AND OPERATION PRINCIPLE

Consider a dual-color TMI combiner (multiplexer) as shown in Fig. 1. The single-mode input and output waveguides are coupled adiabatically to the two-mode waveguide of length L by converging and diverging directional couplers. The two-mode region consists of a higher refractive index central region with approximately doubled index increase, or a wider central region with approximately doubled waveguide width depending upon design considerations. Such a waveguide system can be treated as one structure where two normal modes propagate (one symmetric and one antisymmetric, as sketched in Fig. 1) [12, 13]. The two normal modes propagate through symmetric converging twin waveguides, a two-mode center region, and then a diverging directional coupler with a constant amplitude ratio. However, since the two normal modes have different propagation constants, a phase difference between two modes accumulates as the two

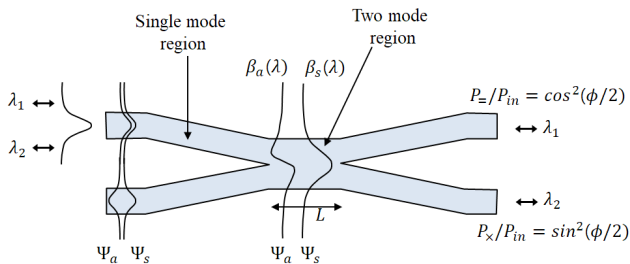


FIG. 1. Dual-color two-mode interference beam combiner (multiplexer).

normal modes propagate through the waveguide system. The output state, after the diverging waveguides are well separated, is determined only by the mode amplitudes (at the output cross section) and the accumulated phase difference ϕ and is given by

$$P_{=} / P_{in} = 2(\alpha_s \alpha_a) \cos^2 \phi / 2 + (\alpha_s - \alpha_a)^2 / 2 \quad (1a)$$

$$P_{\times} / P_{in} = 2(\alpha_s \alpha_a) \sin^2 \phi / 2 + (\alpha_s - \alpha_a)^2 / 2 \quad (1b)$$

where α_s is the relative excitation amplitude of symmetric normal mode ψ_s , and α_a is that of antisymmetric mode ψ_a . If the structure is symmetrical (identical waveguides) and the waveguides are sufficiently separated in the input and output flare, the two mode amplitudes will be nearly identical, i.e., $\alpha_s \cong \alpha_a \cong 1/\sqrt{2}$, when one of two input waveguides is excited. The general discussions for this are given in [12, 13].

The accumulated phase difference ϕ is the sum of that in the converging and diverging region, ϕ_t , and that in the two-mode center region, ϕ_c :

$$\phi(\lambda) = \phi_t(\lambda) + \phi_c(\lambda) \quad (2)$$

where

$$\phi_t(\lambda) = \int_{\text{taper region}} \Delta\beta_t(z, \lambda) dz, \quad \phi_c(\lambda) = \Delta\beta_c(\lambda) L \quad (3)$$

with $\Delta\beta_t(z, \lambda) = \beta_{ts}(z, \lambda) - \beta_{ta}(z, \lambda)$ in the tapering region and $\Delta\beta_c(\lambda) = \beta_{cs}(\lambda) - \beta_{ca}(\lambda)$ in the center region. The accumulated phase difference ϕ depends on wavelength as a result of the different wavelength dependence of the propagation constants of two normal modes. The wavelength dependence comes from the material dispersion of the waveguide material and waveguide dispersion of the two normal modes. Assuming equal excitation of two modes ($\alpha_s = \alpha_a = 1/\sqrt{2}$), we can get

$$P_{=} / P_{in} = \cos^2 \phi(\lambda) / 2 \quad (4a)$$

$$P_{\times} / P_{in} = \sin^2 \phi(\lambda) / 2. \quad (4b)$$

It is possible to control the bar and cross state wavelengths properly by adjusting the length of the two-mode region and the branching angle of the converging and diverging twin waveguides.

III. DESIGN AND SIMULATIONS

As an example of RGB beam combiner design, we consider the cascaded dual-color TMI combiners as shown in Fig. 2. The channel waveguide of square shape is

adopted as a building block of the RGB beam combiner as shown in Fig. 2(a). The width (w_1) and the height of the channel waveguide are $2\ \mu\text{m}$, respectively. The top view of the RGB beam combiner is shown in Fig. 2(b). The refractive index of the quartz cladding is assumed to be wavelength-dependent as follows: [14]

$$n_{clad} = 1.522 - 0.065(\lambda - 0.4). \quad (5)$$

The refractive index of the core glass material is set to be $n_{core} = n_{clad} + 0.015$. The material dispersion effect is incorporated through the use of Eq. (5) and the waveguide dispersion effect is incorporated through the 3-dimensional BPM simulations.

In the lower dual-color TMI combiner, the input and output waveguide center separation (s_1) of the converging and diverging waveguides is $7.2\ \mu\text{m}$ and the length (L_1) of those is $700\ \mu\text{m}$. No straight TMI waveguide is inserted in this case. In the upper dual-color TMI combiner, the input and output waveguide separation (s_2) of the converging and diverging waveguides is $6\ \mu\text{m}$ and the length of those is $700\ \mu\text{m}$. The width (w_2) of the two-mode region is $4\ \mu\text{m}$ and the length (L_2) is $390\ \mu\text{m}$. The size of the combiner is as small as $0.02 \times 3.8\ \text{mm}^2$.

The power transmission versus wavelength from port R to A and from port B to A are calculated using 3-dimensional (3D) beam propagation method (BPM) (RSoft BeamPROP Software) and shown in Fig. 3(a). Red beam ($637\ \text{nm}$) launched into the center input waveguide (port R) and blue beam ($446\ \text{nm}$) into the bottom input waveguide (port B) are shown to be combined into port A. The power transmission versus wavelength from port G to O and from port A to O are calculated using 3D BPM and shown in Fig. 3(b). Green beam ($532\ \text{nm}$) launched into the top

waveguide (port G), and blue ($446\ \text{nm}$) and red ($637\ \text{nm}$) beams into port A are combined into port O.

The overall RGB beam combiner transmission as a function of wavelength are shown in Fig. 3(c), where it is observed that green beam ($532\ \text{nm}$) launched into the input port G, red beam ($637\ \text{nm}$) launched into port R,

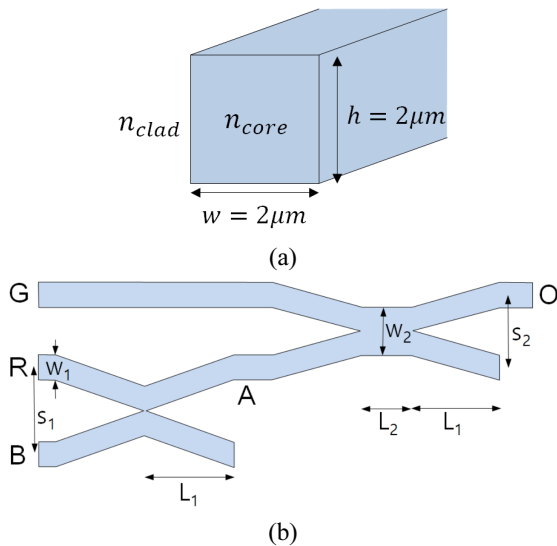


FIG. 2. Schematic view of the proposed red-green-blue beam combiner based on two-mode interference. Two dual-color beam combiners are cascaded.

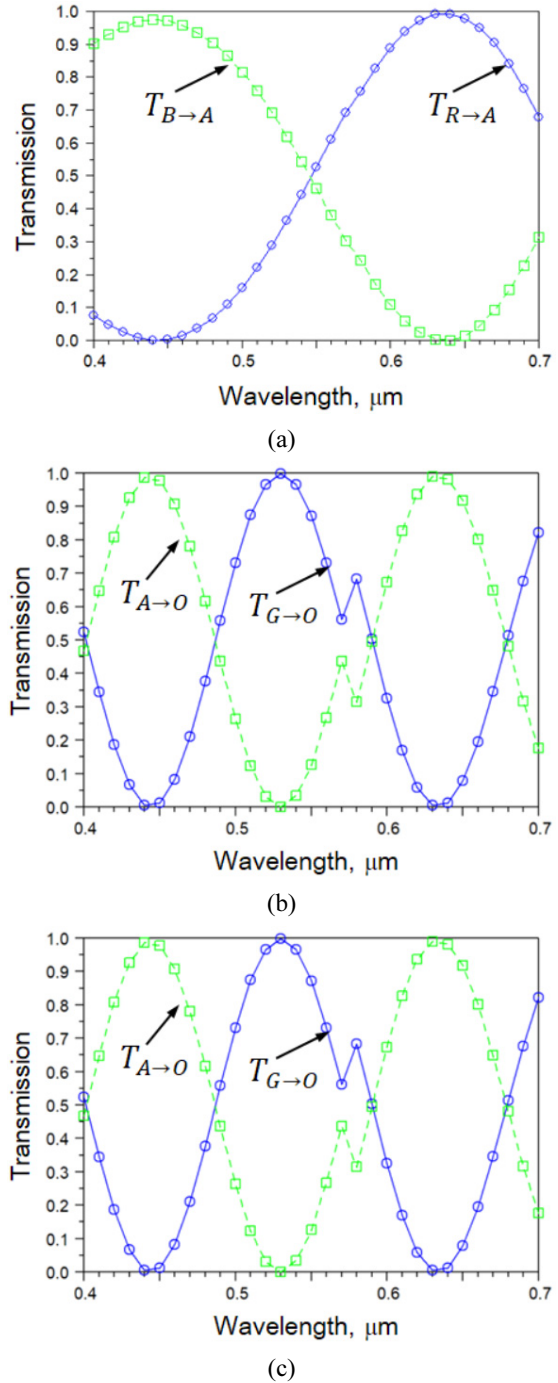


FIG. 3. (a) Power transmissions versus wavelength from port R to A and from port B to A, (b) those from port G to O and from port A to O, and (c) overall RGB beam combiner transmission calculated using 3-dimensional beam propagation method.

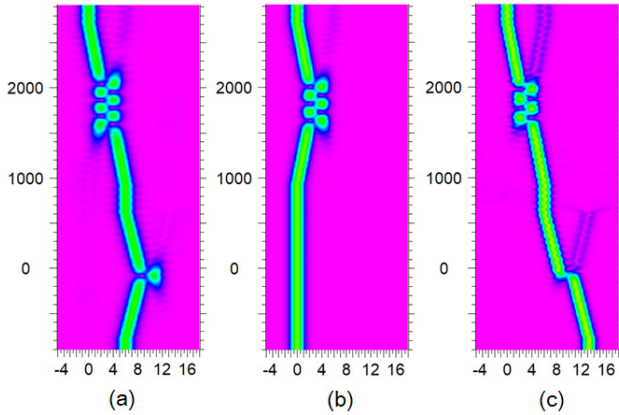


FIG. 4. 3D BPM contour plots for (a) red (637 nm), (b) green (532 nm), and (c) blue (446 nm) beams launched into the corresponding input ports.

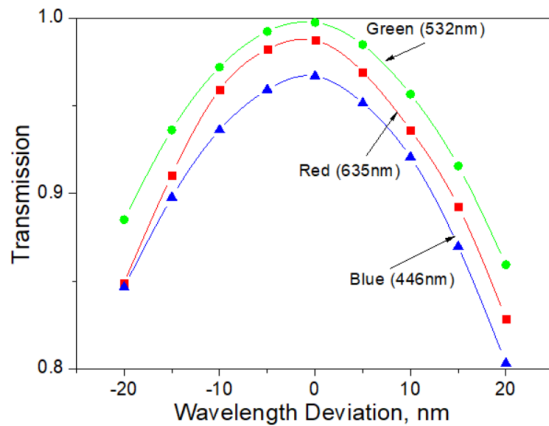


FIG. 5. Enlarged view of peak transmission regions of Fig. 3(c) as a function of wavelength deviation from RGB center wavelengths.

and blue beam (446 nm) launched into port B are shown to be combined through the output port O. The transmissions from the corresponding input ports to the output port at 446 nm, 532 nm, and 637 nm are 0.96, 0.99, and 0.98, respectively. Figure 4 shows the 3D BPM simulation contour plots for the blue, green, and red beams launched into the corresponding input ports. Green, red, and blue beams launched into the three input ports are shown to propagate toward the output port O.

The wavelength of the RGB sources might deviate from the design values for RGB center wavelengths of the RGB combiner and the wavelength tolerance is investigated using 3D BPM calculations. The peak transmission regions of Fig. 3(c) are replotted in detail as a function of wavelength deviation from RGB center wavelengths in Fig. 5. The power transmissions are larger than 90% for the wavelength deviation of ± 10 nm, which indicates quite large wavelength tolerance. In the fabrication process, the waveguide width error might be inevitable and the effect of the width deviation from the design value is also

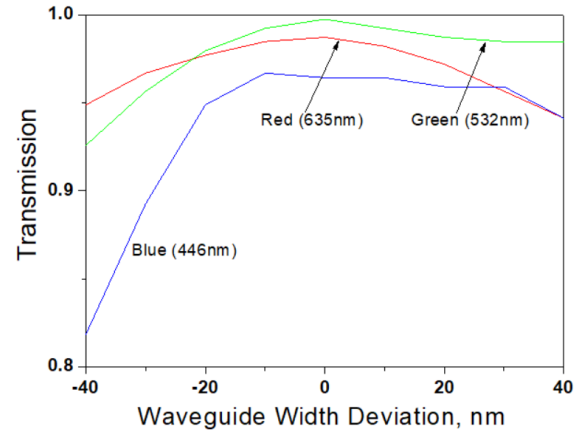


FIG. 6. Variation of power transmissions versus waveguide width error.

investigated. The variation of power transmission for the waveguide width error is shown in Fig. 6. It is observed that the transmissions of all three colors are larger than 94% for the waveguide width deviation of ± 20 nm.

IV. CONCLUSION

A red-green-blue beam combiner is designed simply by cascading two two-mode interference (TMI) beam combiners. In the first stage of the TMI combiner, blue (446 nm) and red (637 nm) beams are combined, and then the two beams are combined with green (532 nm) beam in the second stage TMI combiner. The transmissions from the corresponding input ports to the output port at 446 nm, 532 nm, and 637 nm wavelengths are 0.96, 0.99, and 0.98, respectively. The power transmissions larger than 0.9 are maintained when wavelength deviation is ± 10 nm. When the waveguide width error is 20 nm, the power transmissions for all three colors are larger than 0.94. The size of the combiner is as small as 0.02×3.8 mm². In conclusion, it is shown that a tiny integrated waveguide-type RGB combiner can be simply designed and realized using TMI concept.

ACKNOWLEDGEMENT

The work reported in this paper was conducted during the sabbatical year of Kwangwoon University in 2018.

REFERENCES

1. J. Kimura and M. Takaso, "New markets for projection system and ongoing breakthrough technology," in *Proc. International Display Workshop/Asia Displays (IDW/AD '12)* (Kyoto, Japan, Dec. 2012) **19**, 1355 (2012).

2. J. Pan, S. Tu, C. Wang, and J. Chang, "High efficiency pocket-size projector with a compact projection lens and a light emitting diode-based light source system," *Appl. Opt.* **47**, 3406-3414 (2008).
3. M. Billingham and T. Starner, "New ways to manage information," *Computer* **32**, 57-64 (1999).
4. H. Tamura, "Steps toward a giant leap in mixed and augmented reality," in *Proc. International Display Workshop/Asia Displays (IDW/AD '12)* (Kyoto, Japan, Dec. 2012) **19**, 7 (2012).
5. S. Kim and E. Kim, "A novel configuration of LCD projectors for efficient orthogonal polarization of two projected views," *Opt. Commun.* **266**, 55-66 (2006).
6. J. Miller, S. J. Woltman, and T. Byeman, "Laser based scanned beam display system," in *Proc. 1st Laser Display Conference (LDC'12)* (Yokohama, Japan) LDC6-2, 25-27 (2012).
7. Oculus VR, LLC., Oculus rift. <https://www.oculus.com/rift/> (Date of access: 08/08/2018) (2015).
8. Samsung Electronics, Ltd., Samsung Gear VR. <http://www.samsung.com/global/galaxy/gear-vr/> (Date of access: 08/08/2018) (2015).
9. Y. Tanahashi, O. Kasono, T. Yanagisawa, T. Nomoto, I. Kikuchi, T. Ezuka, K. Nakamura, H. Takahashi, Y. Imasaka, Y. Tsuchida, and T. Shimizu, "Development of full-color laser head-up display," in *Proc. International Display Workshop/Asia Displays (IDW/AD '12)* (Kyoto, Japan, Dec. 2012) **19**, 1987-1990 (2012).
10. O. Utsuboya, T. Shimizu, and A. Kurosawa, "40.1 invited paper: augmented reality head up display for car navigation system," in *Proc. SID Symposium Digest of Technical Papers* **44**, 551-554 (2013).
11. A. Nakao, R. Morimoto, Y. Kato, Y. Kakinoki, K. Ogawa, and T. Katsuyama, "Integrated waveguide-type red-green-blue beam combiners for compact projection-type displays," *Opt. Commun.* **330**, 45-48 (2014).
12. R. A. Forber and E. Marom, "Symmetric directional coupler switches," *IEEE J. Quantum Electron.* **QE-22**, 911-919 (1986).
13. Y. Chung, J. C. Yi, S. H. Kim, and S. S. Choi, "Analysis of a tunable multichannel two-mode-interference wavelength division multiplexer/demultiplexer," *IEEE J. Lightw. Technol.* **7**, 766-777 (1989).
14. M. Khashan and A. Nassif, "Dispersion of the optical constants of quartz and polymethyl methacrylate glasses in a wide spectral range: 0.2-3 μm ," *Opt. Commun.* **188**, 129-139 (2001).